

1 **Upgrading fluidised bed bioreactors for treating brewery wastewater by using** 2 **a fluid-like electrode**

3 Yeray Asensio^{1*}, María Llorente¹, Patricia Fernández², Sara Tejedor-Sanz¹, Juan Manuel Ortiz³,
4 Juan Francisco Ciriza², Víctor Monsalvo⁴, Frank Rogalla⁴, Abraham Esteve-Núñez¹.

5 ¹University of Alcalá, Department of Chemical Engineering, Ctra. Madrid-Barcelona, km 33,6, 28871, Alcalá de
6 Henares, Madrid, Spain.

7 ²Mahou-San Miguel, C. Titán 15, 28045, Madrid, Madrid, Spain.

8 ³IMDEA-WATER Institute, Punto Com 2, 28805, Alcalá de Henares, Madrid, Spain.

9 ⁴FCC AQUALIA, Department of Innovation and Technology, Avda. del Camino de Santiago 40, Madrid, Madrid,
10 Spain.

11 *corresponding author: Yeray Asensio. E-mail: yeray.asensio@uah.es

12 **Abstract**

13 Anaerobic digestion has historically shown critical operational limitations for treating industrial
14 wastewater. Our work aims to evaluate the resilience capacity of a novel concept so-called
15 microbial electrochemical-fluidised bed reactor (ME-FBR) for treating real brewery wastewater
16 under continuous operation mode over one year period. All assays were run in parallel using a
17 conventional anaerobic fluidised bed reactor (AFBR). The resilience tests were designed attending
18 to the most typical operational problems showed by the AFBR technology in real brewery
19 wastewater treatment plants. Four different stress situations were tested: i) pollutants overloading
20 (as high as 51.2 kgCOD/m³ d), ii) presence of an active biocide in the fed stream (5% v/V), iii)
21 operation of the reactors after long starvation periods (16 days) and iv) operation at low
22 temperature (<25°C). Our pre-pilot scale ME-FBR outperformed traditional AFBR for wastewater
23 treatment capacity under all stress test regarding COD removal rate, total nitrogen (TN) removal
24 rate and bioenergy recovery (bioelectrochemical-assisted hydrogen generation). Among all stress
25 test, low temperatures and long starvation periods deeply decrease the robustness of both
26 technologies.

27

28 **Keywords:** Microbial electrochemistry; anaerobic fluidised bed reactor; anaerobic digestion;
29 electroactive bacteria; brewery wastewater

31 **1. Introduction**

32 Anaerobic digestion (AD) and Anaerobic Fluidised Bed Reactors (AFBR) are currently the most
33 widely installed secondary treatments in industrial wastewater treatment plants (WWTP) for
34 treating high-strength wastewaters due to its capacity to generate methane, providing a potential
35 for energy generation while producing low surplus sludge respecting aerobic treatments [1–3]. In
36 spite of being designed attending to the coarse experience gained during the last 100 years, AD
37 has historically showed some critical operational limitations. Some of those well identified
38 operational problems are i) high concentration of nutrients, specially nitrogen and phosphorous in
39 the effluent [4–7], ii) low capacity to treat wastewater at low temperatures [8,9], iii) instability of
40 the technology under high organic loads in the fed stream [10–12], iv) low COD removal rates
41 after starving periods [13,14] and v) microorganism inhibition with the presence of biocides
42 extensively used in the brewery industry as cleaning agents [15,16]. The increase of the matrix
43 complexity in industrial wastewater during the last years demands to explore new strategies to
44 increase the robustness of such treatment systems.

45 In that sense, Microbial electrochemical technologies (MET) represent a promising field to
46 overcome the well-known limitations of conventional AD technologies [17–22]. These
47 technologies are based on the capacity of electroactive bacteria to exchange electrons with
48 electrically conductive materials [23,24]. In some MET, electroactive bacteria act as a natural
49 catalyst for oxidizing the organic pollutants present in wastewater, then transferring electrons to
50 the electrode so green bioenergy (eg. electrical power, hydrogen, methane) can be harvested [25–
51 27]. The electrons accepted by the electroconductive material (anode) are then transferred i) to the
52 cathode material by an external electric circuit for generating power in devices called microbial
53 fuel cells (MFC) [23,28–30], or ii) to a counter electrode, under potentiostat control, in devices
54 called microbial electrolysis cell (MEC) [31–34]. So, both MFC and MEC have been extensively
55 tested during the last decades as promising industrial wastewater treatments at lab-scale [35–40]

56 Nevertheless, even if at laboratory scale results are promising, scaling-up this technology is a huge
57 handicap due to a limited electrode surface area where redox reactions take place and,
58 consequently, a mass transfer limitation between substrates and microorganisms [41]. Such
59 problems associated to the use of static biofilm-based electrodes have proposed to be overcome by

60 a novel concept where the classical static electrode is replaced by a fluid-like electrode made of
61 electroconductive carbon microparticles [42–44]. Indeed, the proof of concept raised a device so-
62 called Microbial Electrochemical Fluidized Bed Reactor (ME-FBR) that was applied to treat
63 industrial wastewater from the brewery sector. Actually, the advantage of using ME-FBR has
64 been already reported regarding available electrode surface, decrease in cell wash-out, and
65 enhancement of mass transfer [45,46]. The concept of using a fluidised anode serving as electron
66 acceptor for electroactive bacteria achieved up to 87% removal of the total COD contained in the
67 wastewater [42], and revealed a process of extremely high coulombic efficiency. In addition,
68 polarization of the fluidized electrode favored the removal of total nitrogen and total phosphorus
69 (46% and 50%, respectively), what implies a realistic operational advantage respecting the
70 conventional biologic treatments [42]. Furthermore, a recent application has demonstrated that
71 ME-FBR can operate with the fluidized bed acting as electron donor to promote reductive
72 metabolism by electroactive bacteria in low COD medium (eg. denitrification) and, additionally,
73 produce biohydrogen (Tejedor et al., 2020).

74 Electroactive bacteria commonly interact with electrodes directly by forming a biofilm.
75 Actually, *Geobacter* species have been reported to dominate the microbial communities found in
76 anodes composed of mixed populations [47–49]. This genus has also been identified in the
77 granules of an upflow anaerobic sludge blanket (UASB) reactor treating brewery waste [50]. In
78 spite of the absence of an electrode, *Geobacter* was found to perform direct extracellular electron
79 transfer (DEET) by exchanging the electrons with methanogenic communities, through direct
80 interspecies electron transfer (DIET). Specifically, *Methanosarcina barkeri* has been shown to be
81 capable of performing DIET in co-cultures with *Geobacter* species [50,51]. DIET can also take
82 place with a mineral as a mediator, a process in which different species use as conduits of electrons
83 nano-mineral particles or conductive surfaces such as activated carbon granules or biochar [52,53].
84 This phenomena has also been described to stimulate methane production and *Geobacter* growth
85 [45,50,54,55]. All these findings suggest that co-aggregation of *Geobacter* species and
86 methanogens may be a common phenomenon in methanogenic environments and that might be
87 relevant with respect to methane production in anaerobic digesters.

88 In this context, the goal of this work has been to evaluate the resilience capacity for AFBR
89 and ME-FBR technologies for treating real brewery wastewater during one-year period. The stress

90 tests have simulated most typical operational problems for conventional operation of AD in
91 industrial WWTPs; COD overloads, biocide dosing, starving periods and operation under low
92 temperatures (<25°C).

93

94 **2. Materials and methods**

95 *2.1. Design of the Microbial electrochemical-fluidised bed reactor (ME-FBR) and the anaerobic* 96 *fluidized bed reactor (AFBR).*

97 The set-ups used in this work consisted of two membrane-less pre-pilot reactors, ME-FBR
98 and AFBR. They were evaluated regarding the wastewater treatment capacity during several
99 resilience tests.

100 The pre-pilot ME-FBR and AFBR units were designed and assembled in methacrylate with
101 a tubular geometry. Both reactors were equipped by a flux distributor at the bottom zone in order
102 to assure the fluidisation of the sewage sludge and the electro-conductive anode material though
103 the column, such distributor was key to avoid dead zones, capable of affecting the efficiency in
104 the wastewater treatment. The top zone of both reactors was sealed with a gas collector in order to
105 periodically (every two days) monitor the biogas and hydrogen generation by a portable biogas-
106 analyser (Dräger X-am[®] 5000, Germany). In addition, five sampling ports were installed at
107 different heights over the tubular structure. The main structural difference between the ME-FBFR
108 and the AFBR was the presence of two additional sampling ports on the ME-FBR to host the
109 electrochemical probes, one on the bottom zone and the other on the top zone. The working volume
110 of the ME-FBR and AFBR was 5.4 L, including the recirculation pipe and the bed volume.

111 Despite de similarity in geometrical design, the difference between the AFBR and ME-
112 FBR was due the integration of electrodes (anode and cathode) in the last one. The anode material
113 in ME-FBR was made of electroconductive activated carbon (20% v/V, Aquasorb[®], Germany).
114 This electroconductive activated carbon accepted the electron transfer from the microbial biofilm
115 and, eventually transferred such electrons to the conductive anode collector. Additionally, this
116 material showed a high porosity that highly favour the microorganism's growth on its surface. The
117 anode collector was a graphite plate (4.5 cm x 4.5 cm) vertically immersed in the fluidising bed.
118 A stainless-steel sponge was equipped as cathode material.

119 *2.2. Experimental procedure of resilience tests*

120 The resilience tests were conducted to simulate i) two high organic loading rates (27.2
 121 kgCOD/m³ d and 51.2 kgCOD/m³ d), ii) a biocide dosing based on quaternary amines normally
 122 used to clean the industrial equipment (didecyldimehtylammonium chloride – DDAC), iii) a
 123 starving period and, finally, iv) operation under low temperature (25°C) Table 1. The resilience
 124 tests were performed independently and consecutively, always waiting for the systems to be
 125 recovered and stabilized from the previous disruption test.

126

Table 1. Conventional AFBR and ME-FBR long-term operation. Resilience test descriptions and monitored parameters.

Resilience test	Operation time (d)	Monitored parameter
No resilience tests (Standard operation of AFBR and ME-FBR)	1 – 31 39 - 52	COD removal, biogas hydrogen generation, pe generation, nutrients ren
COD overloads	32 -38 53 -59	COD consumption rate, t and hydrogen generati
Biocide dosing	73 -79	TN consumption rat
Starvation period	88 - 110	COD removal
Low temperature	306 -340	COD removal

127

128 *2.3 Electrochemical control and operation*

129 A potentiostat (NANO-ELECTRA NEV3, Spain) was connected to the electrodes to
 130 polarize the anode material at 0.6 V (versus Ag/AgCl) during the operation of the ME-FBR. The

131 presence of two reference electrodes (Ag/AgCl 3 M KCl – HANNA Instruments, Germany)
132 allowed to monitor the cathode and cell potentials during the continuous operation of the reactor.
133 Nevertheless, the AFBR was not equipped with any potentiostat since such reactor was free of
134 electroconductive material.

135 Both pre-pilot reactors were fed in continuous mode by a peristaltic pump (Watson Marlow
136 205S, United Kingdom); moreover, fluidization was achieved by using two additional peristaltic
137 pumps (Heidolph 5006, Germany), one for each reactor. They operated to favour a recirculation
138 flow from the top section to the flow distributor hosted in the bottom zone. Both reactors were
139 operated with a hydraulic retention time (HRT) of 9 h. Sampling and analysis were performed
140 daily.

141 *2.4. Inoculum and real wastewater*

142 Activated anaerobic granular sludge from an industrial wastewater treatment plant of a
143 brewery WWTP (Alovera, Guadalajara, Spain) was used as inoculum for both reactors. Both
144 bioreactors were fed by (1:1 v/v) activated sludge from chemical coagulated wastewater. This
145 start-up phase took seven days under both semi-continuous mode and anoxic conditions to favour
146 the formation of electroactive and anaerobic communities for ME-FBR, and just anaerobic ones
147 for the AD-FBR. After this period both reactors were fed in continuous mode with real wastewater
148 from the brewery plant using a peristaltic pump (Watson Marlow 205S) with a fixed flowrate of 1
149 L/h.

150 *2.5. Chemical and Physical-chemical analysis*

151 COD concentration and nutrient, total nitrogen and total phosphorous, concentrations were
152 determined using commercial colorimetric probe tests (HACH – LCK cuvette tests, Germany)
153 digested in a commercial HACH digester (HACH ref. DRB-201B, Germany) and measured on a
154 spectrophotometer analyser (HACH ref. DR1900, Germany). Finally, pH and conductivity were
155 measured by a multiparametric probe (HACH ref. HQ40D, Germany).

156

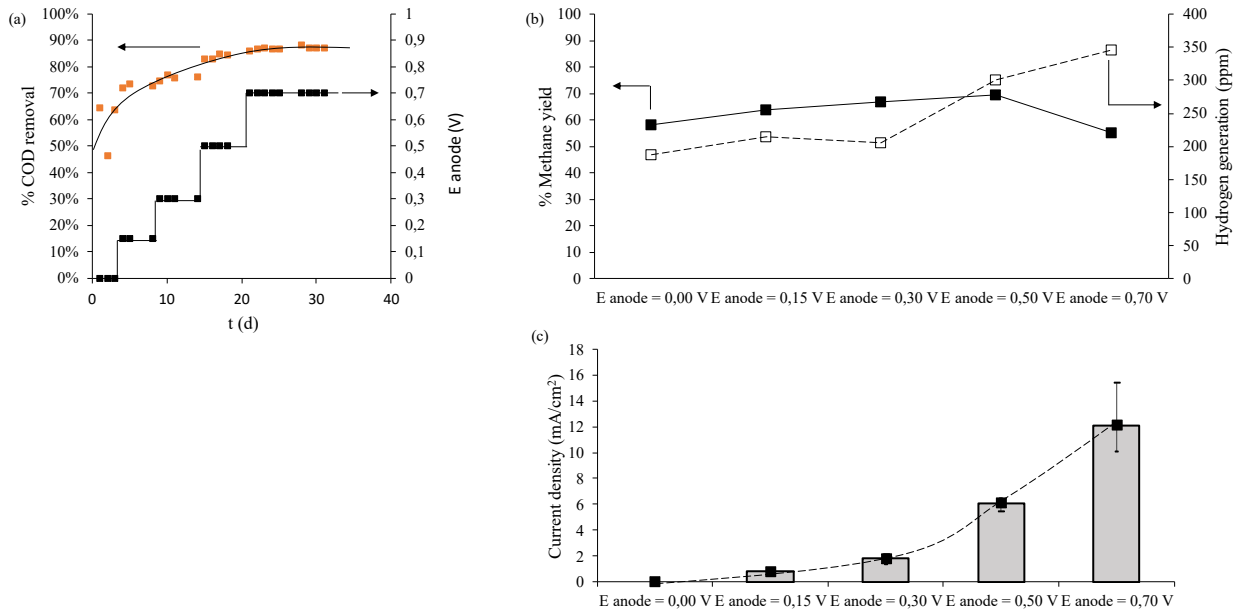
157 **3. Results and Discussion**

158 The most standard methodology for treating brewery wastewater is to conduct an anaerobic
159 biological treatment. In the current study such technology is represented by an Anaerobic
160 Fluidised-bed reactor that will be our reference system to explore the capacity of a new design so-
161 called microbial electrochemical fluidized-bed reactor.

162 3.1. The performance of a Microbial Electrochemical Fluidized Bed Reactor (ME-FBR)

163 An initial characterization of the ME-FBR was performed in order to validate the efficiency
164 of the new approach regarding COD removal, biogas generation and electrochemical-assisted
165 hydrogen production with real brewery wastewater. The strategy after the ME-FBR configuration
166 was based on enhancing the oxidative metabolism by using a fluid-like electroconductive material
167 acting as terminal electron acceptor in microbial respiration. The electrochemical nature of such
168 electron acceptor allowed a control of the redox potential of the bed. Indeed, the first parameter to
169 be evaluated was the impact of such polarization potential in the COD removal. Not surprisingly,
170 the COD removal increased from 60% COD removal at 0,15 V to 87% under a polarization of 0,7
171 V. Thus, the behavior of COD removal (see Fig.1.a) suggested that microbial oxidation of organic
172 matter is limited by mass transfer, and not by electron transfer, as COD removal is directly related
173 to oxidation current in the anode. So, by using ME-FBR is possible to overcome one of the main
174 problems related to MET devices as indicated previously, namely, low overall current for practical
175 treatment uses. Thus, anode potentials higher than 0.7 V would not reach better performance
176 despite investing more energy in polarizing. On top of that, it seems reasonable to avoid such a
177 high redox potential that could damage molecules from membrane bacteria.

178



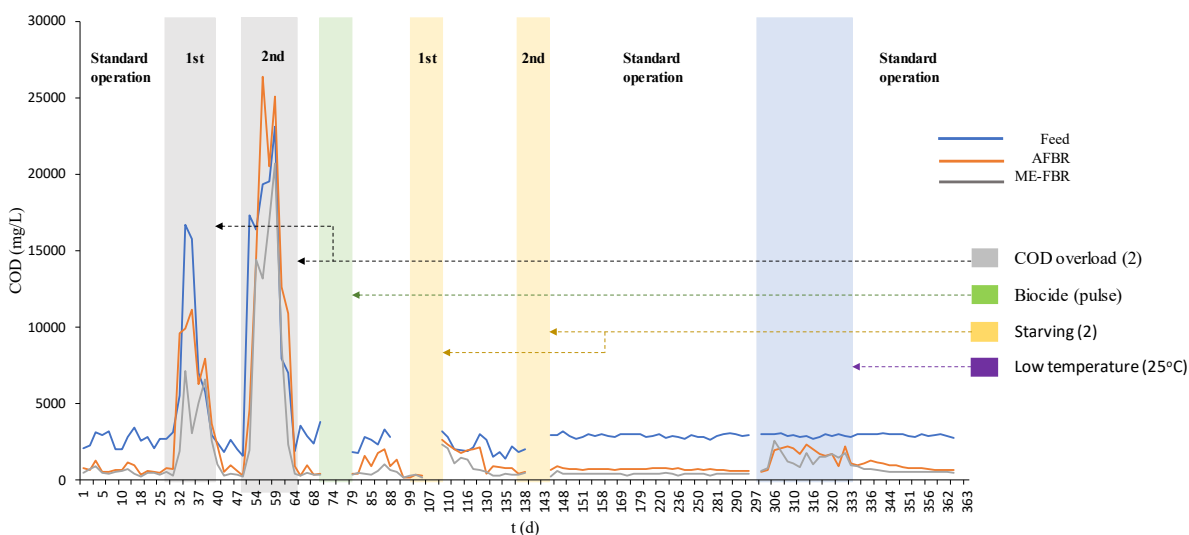
179
 180 **Fig.1.** ME-FBR characterization. (a) Influence of the anode polarization (V) on the % COD
 181 removal. Symbols: (■) % COD removal, (■) Anode polarization, E (V vs Ag/AgCl). (b) Methane
 182 and hydrogen production in the ME-FBR reactor. Symbols: (■) Hydrogen concentration in the
 183 produced biogas (mg/L). (c) Current density obtained in the ME-FBR. Symbols: (■) Output
 184 current density (mA/cm²).

185 On top of removing COD from wastewater, a ME-FBR constitutes by itself a device for
 186 generating biogas. In contrast with standard anaerobic bioreactors where organic matter is
 187 converted into CH₄ and CO₂, the electrochemical nature of ME-FBR allows the production of
 188 hydrogen at the counter electrode (cathode, water reduction reaction, $2\text{H}_2\text{O} + 2\text{e}^- \rightarrow \text{H}_2 + 2\text{OH}^-$,
 189 $E^\circ = -0.83\text{ V}$). Interestingly, all the electrons reducing water on the surface of the cathode were
 190 originally transferred to the anodic bed by electroactive microbial oxidation of COD (as anode
 191 potential is significantly lower than redox potential for water oxidation, $\text{O}_2 + 4\text{H}^+(\text{aq}) + 4\text{e}^- \rightarrow$
 192 $2\text{H}_2\text{O}$, $E^\circ = 1.23\text{ V}$). Moreover, the methane concentration in the biogas did not varied substantially
 193 (Fig 1.B), while the hydrogen concentration rapidly increased when the anode potential was set in
 194 the range 0.5 – 0.7 V, achieving a maximum hydrogen generation at 0.7 V. This increase in the
 195 hydrogen generation at higher anode potentials was also correlated with the higher current density
 196 (Fig.1. c) harvested by the system (2.24 A/m³, referred to anode fluidized bed volume).

197 3.2. ME-FBR versus AFBR: exploring the limits

198 Conventional anaerobic digesters for treating wastewater from the brewery industry must deal
 199 with a well-known set of operational problems (e.g. overload, biocide, starving, low temperature).
 200 Our first target was to perform a series of resilience tests in order to compare the robustness of
 201 both technological solutions, ME-FBR and AFBR, using chemically coagulated wastewater from
 202 a brewery plant. Interestingly, the analysis of such wastewater revealed a complex feeding stream
 203 marked by its variability, mainly high content of COD, total nitrogen (TN) and total phosphorous
 204 (TP). Furthermore, the comparative study was monitored for one year, evaluating the long-term
 205 operation of the conventional AFBR and ME-FBR (Figure 2).

206

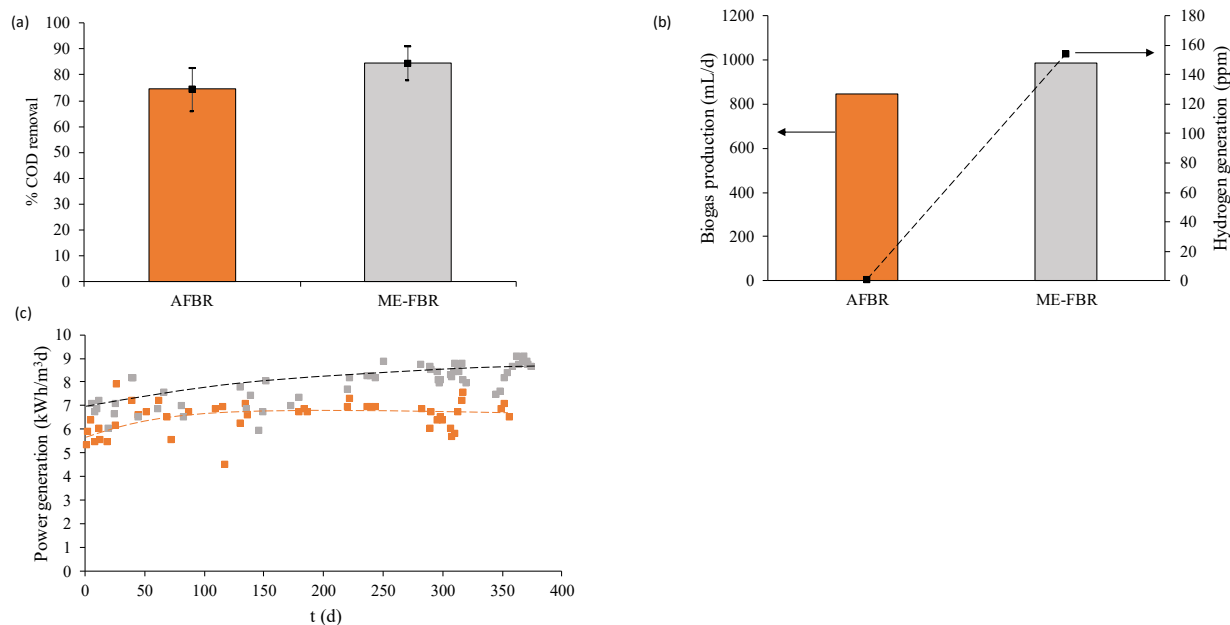


207

208 **Fig.2.** Long-term operation of the AFBR and ME-FBR for one year. Description of the resilience
 209 tests. (-) Influent COD concentration at influent (mg O₂/L), (-) COD concentration of the AFBR
 210 effluent (mg O₂/L), (-) COD concentration of the ME-FBR effluent (mg O₂/L).

211 Our first attempt was to explore the robustness of ME-FBR and AFBR for treating real
 212 brewery wastewater as a key baseline for further disruption effects. The operation of both
 213 technologies in terms of %COD removal, biogas generation and power production were performed
 214 using the same feeding stream (Figure 3).

215



216
 217 **Fig.3.** ME-FBR and AFBR operation during standard operation. **(a)** AFBR (orange bar) and COD
 218 removal for ME-FBR (grey bar). **(b)** Biogas generation and hydrogen concentration. Symbols: (■)
 219 Hydrogen concentration on the enriched biogas (mg/L). **(c)** Energy generation of the ME-FBR and
 220 AFBRD reactor during standard operation associated to biogas production. Symbols: (■) ME-FBR
 221 (kWh/m³ d), (■) AFBR (kWh/m³ d).

222
 223 During the standard operation, ME-FBR outperformed AFBR for COD removal by up to
 224 10%. The higher efficiency of ME-FBR for treating wastewater was directly related to the anode
 225 polarization and indeed to the activity of electroactive bacteria. Such an increase in COD oxidation
 226 favored biogas generation (984 mL/d) including a high hydrogen concentration (154 mg H₂/L),
 227 that notably increased the net power generation in respect to the conventional AFBR (Fig.2. c).
 228 Moreover, the net energy applied to the electroconductive bed was negligible in comparison with
 229 the high net energy produced by the reactor.

230 Once the standard operation was tested for AFBR and ME-FBR reactors, the resilience
 231 capacity of both technologies under COD overload was performed. Two different COD overloads
 232 (27.20 and 51.20 kgCOD/m³ d) were evaluated for one week period each (Table 2).

233

Table 2. OLR (kgCOD/m³ d) and HRT (h) during the two COD overloads applied to the conventional AFBR and ME-FBR reactors

	Operation time (d)	OLR (kgCOD/m ³ d)	HRT (h)
Standard operation	1 -31	7.10	9
	39 – 52	6.00	9
COD overload 1	32 -38	27.20	9
COD overload 2	53 – 59	51.20	9

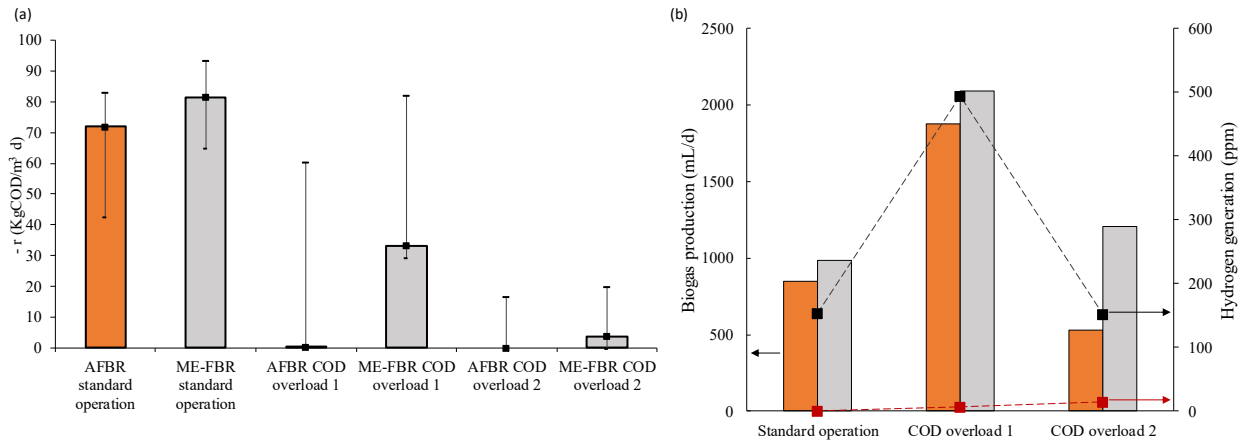
234

235 The wastewater treatment capacity under this first disruptive test was measured in terms of
 236 COD removal rate. AFBR was severely affected by high concentrations of COD, actually reducing
 237 the treatment capacity of the system from 71.9 kgCOD/m³ d to 0.23 kgCOD/m³ d during the first
 238 COD overload (Fig. 4). Such decrease was observed not just as accumulation of organics in
 239 effluent but also as an increase in values from error bars (Fig.4.a). This negative effect was greatly
 240 intensified with the second COD overload when the conventional AFBR was not able to consume
 241 COD, mainly due to VFA accumulation, which eventually inhibited the hydrolytic bacteria
 242 responsible for the first step of conventional anaerobic digestion. In contrast, ME-FBR validation
 243 for COD removal outperformed AFBR by 30-fold after the first overload and 55-fold after second
 244 overload. The higher stability of ME-FBR could be observed in low values for error bars (Fig 4.a).
 245 So, the anode polarization in ME-FBR favored the oxidation of organic pollutants, even supporting
 246 high VFA removal rates avoiding critical operational problems as pH depletion normally observed
 247 in AFBR technology.

248 The biogas production after first COD overloading resulted in an increase of flow rate by 2-fold
 249 as a general trend for both AFBR and ME-FBR. Such situation was not kept after a more severe
 250 COD overloading resulting in a flow rate for AFBR even lower than shown in the pre-overloading
 251 situation. In contrast, ME-FBR flow rate was not affected after overloading COD by 8-fold. VFA
 252 accumulation in AFBR is a typical situation of destabilization, due to hydrolytic bacteria
 253 inhibition, leading to a critical decrease on the biogas generation. Actually, very little
 254 concentration of hydrogen was detected in AFBR (14 mg H₂/L), suggesting an increase in the

255 partial fermentation of the accumulated organic compounds. In contrast, the cathode-based
 256 generation of hydrogen increased resulted in biogas hydrogen percentage as high as 500ppm.

257



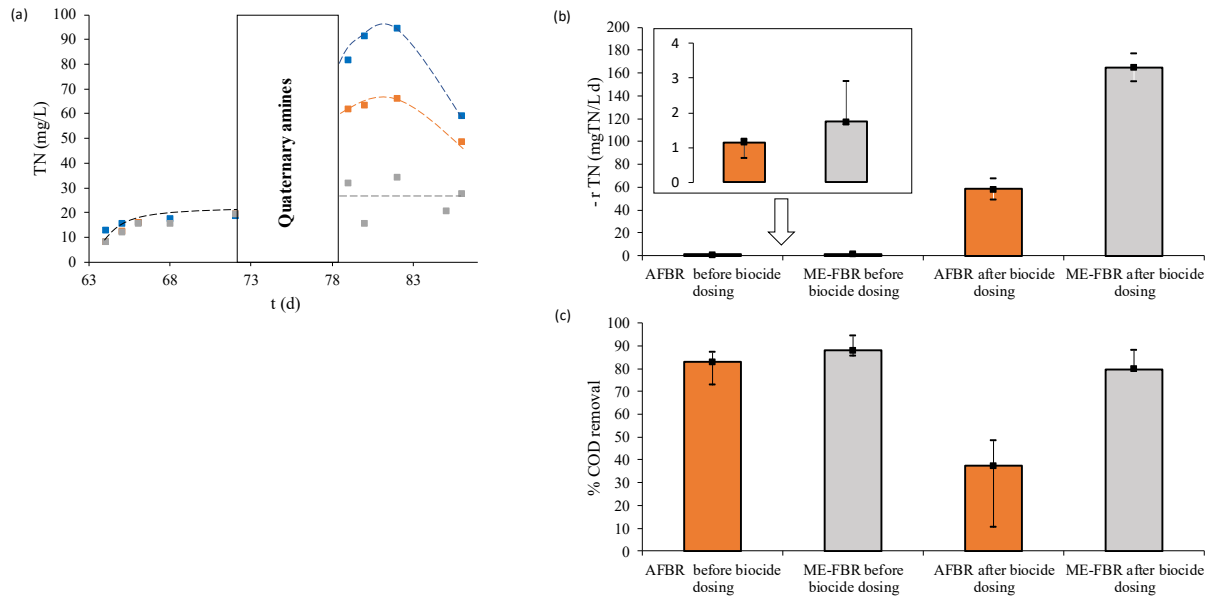
258

259 **Fig.4.** COD removal rate under COD overloads of the AFBR and ME-FBR technologies. **(a)** COD
 260 removal rates of AFBR and ME-FBR reactors. **(b)** Biogas generation and hydrogen production.
 261 Symbols: (■) Hydrogen production during the ME-FBR operation (mg/L), (■) Hydrogen
 262 production during the AFBR operation (mg/L).

263

264 The presence of very high-effective biocides for cleaning purposes is frequent in the food
 265 and brewery industry. The main problems associated to these active molecules are related to their
 266 complex structure and their recalcitrant nature. Both inherent characteristics exacerbates the
 267 difficulty for removing their traces after use in conventional primary and secondary treatments
 268 from common industrial WWTP. Attending to this problem, the capacity of the AFBR and ME-
 269 FBR to remove the most typical biocide used in the food and brewery industry was evaluated. The
 270 resilience capacity of the systems to remove this product was monitored attending to the total
 271 nitrogen removal rates associated to both systems when a biocide was dosed in continuous mode
 272 for six days as observed (Fig.5).

273



274

275 Fig.5. TN concentration, TN removal rates, and COD removal for AFBR and ME-FBR reactors
 276 during a biocide resilience test. (a) TN concentration. Symbols: (■) TN concentration in the feed
 277 stream (mg/L), (■) TN concentration in AFBR effluent (mg/L), (■) TN concentration in ME-
 278 FBR effluent (mg/L). (b) TN removal rate for AFBR and ME-FBR reactors before and after the
 279 biocide dosing. (c) COD removal for AFBR and ME-FBR reactors before and after the biocide
 280 dosing.

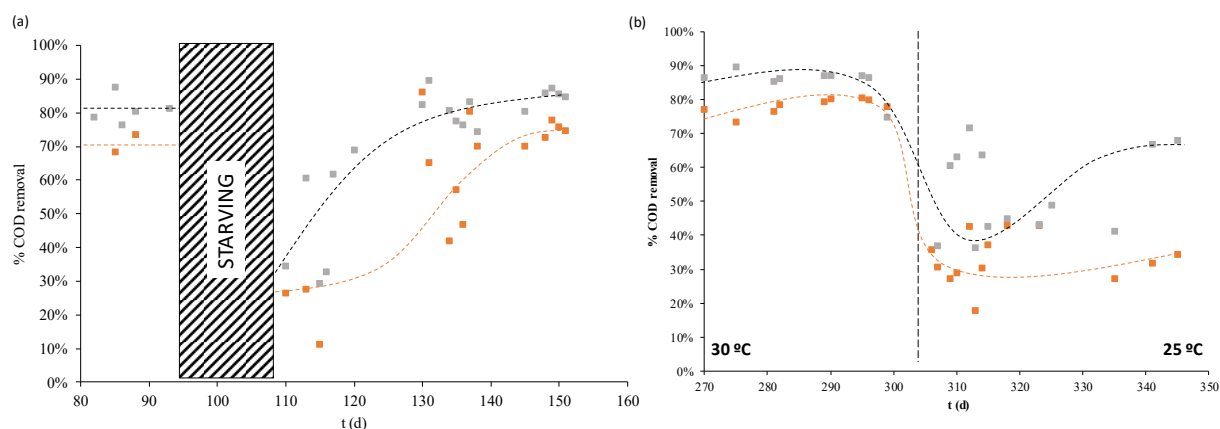
281

282 The resilience test for ME-FBR revealed a lack of inhibition in terms of nitrogen removal after the
 283 biocide dosing (Fig.5.a). In contrast, AFBR was severely affected and TN concentration in the
 284 effluent increased from 20 mg/L to 66 mg/L, while TN removal rate was ca. 30% of the one shown
 285 by ME-FBR. In addition, a marked decrease on COD removal was shown by the AFBR after the
 286 biocide dosing, from 83% to 37%, while biocide did not have major impact in COD removal for
 287 ME-FBR (Fig 5.c). Despite the anoxic conditions, the ME-FBR revealed an unexpected high
 288 nitrogen removal (70%); the rationale after such finding could be the microbial electrochemical
 289 oxidation of nitrogen compounds to nitrate in the anodic particles, and subsequent nitrate reduction
 290 by anaerobic suspended microorganisms using organic matter as electron donor.

291 Finally, the stress response after a starvation period of 16 days and low temperature (25°C) was
 292 evaluated. The resilience tests attending to the % COD removal revealed a severe decrease (ca.

293 70%) for both systems just after the starvation period (Fig.6). Nevertheless, the recovery period in
 294 the case of the ME-FBR was just 20 days of operation, in contrast with the 40 days necessary to
 295 recover the standard capacity for AFBR. In a similar way, a temperature drop, from 35°C to 25°C
 296 had a dramatically reduction of in COD removal (ca. 40-50%) for both systems. However, ME-
 297 FBR microbial community readapted to low temperature after one month of operation to reach
 298 70% COD removal in contrast with AFBR that unable to remove more than 30% of the COD. The
 299 buffer capacity of the ME-FBR in respect to AFBR during starvation and low temperatures was
 300 due to the selective advantage achieved by applying a constant anode potential to stimulate
 301 electroactive bacteria.

302



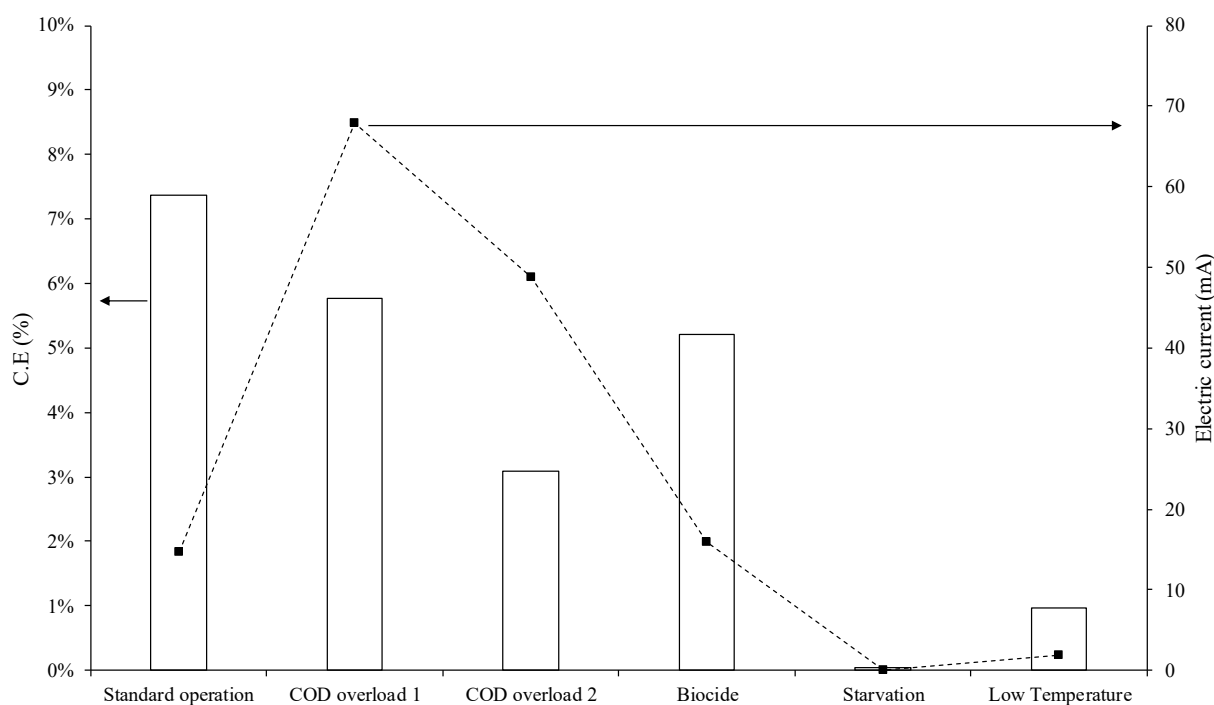
303

304 **Fig.6.** Resilience capacity of the AFBR and ME-FBR reactors during starving step and under low
 305 operational temperatures (25°C). **(a)** % COD removal after staving. Symbols: (■) AFBR, (■) ME-
 306 FBR. **(b)** % COD removal under the operation of the systems at low operational temperatures
 307 (25°C). Symbols: (■) AFBR, (■) ME-FBR

308 The basic microbial electrochemical parameters of the ME-FBR reactor were monitored
 309 during the long-term operation to obtain physiological information on real time that complement
 310 the standard data based on COD removal. The complete inhibition of electroactive bacteria was
 311 observed at low temperatures and after long starvation periods (Fig.7). This inhibition was checked
 312 attending to the very low current densities during those disruptive periods, 2.5×10^{-3} mA after the
 313 starvation period and 1.1 mA at low temperatures. Those low current densities were directly related
 314 to the low coulombic efficiencies (CE) achieved during those periods, being 0.04% after the

315 starvation time and 0.97% during the operation at 25°C, revealing a severe inhibition of
 316 electroactive bacteria. CE referred to the rate of total organic matter in the wastewater that is
 317 converted into electricity by electrogenic microorganisms, and eventually harvested as current
 318 flow, over the total amount of electrons obtained from the organic matter oxidation. Furthermore,
 319 ME-FBR technology resulted highly capable of treating biocide-supplemented wastewaters
 320 attending to the bioelectrochemical parameters, current density and CE, which were quite similar
 321 in respect to the conventional operation of the reactor (3.0 A/m³ and 5.7%, approximately).

322



323

324 **Fig.7.** Basic electrochemical parameters of the ME-FBR. Average electric current of the ME-FBR
 325 technology during the different resilience tests and related CE (%). Symbols: ■ Electric current
 326 (mA)

327 The increase of COD in the influent has a direct influence on both the current density and
 328 CE (Fig.7). During the first COD overload (27.2 kgCOD/m³ d) the current density was increased
 329 by 6-fold. Such results indicated the fast adaptability of electroactive bacteria at high COD
 330 overloads. Nevertheless, very high COD concentrations in the feeding stream (51.2 kgCOD/m³ d)
 331 led to a smooth current efficiency drop in respect to the first COD overload. Nevertheless, the high

332 increase on the inlet COD did not really affect the electroactive bacteria according to the high
333 current densities achieved (9.19 A/m³). Nevertheless, it should be considered that the experimental
334 work has been performed in an industrial environment with real wastewater. However, since our
335 research has been conducted at pre- pilot scale, additional activities should be performed in order
336 to scale-up ME-FBR technology for treating industrial wastewater.

337

338 **4. Conclusions**

339 This study demonstrates that ME-FBR outperforms AFBR either under standard operational
340 conditions or under stress operational tests (COD overload, biocide dosing, long starvation periods
341 and operation at low operational temperatures). In steady state, ME-FBR increases the wastewater
342 treatment capacity in 10% compared to AFBR with an organic loading rate (OLR) of 6.0-7.1 kg
343 COD/m³ d, as well as an increase of 30% related to the energy production associated to generated
344 biogas. Our results clearly revealed why polarizing a fluidized-electrode shows a direct impact on
345 COD and TN removal, avoiding inhibition phenomena typically observed in standards systems
346 like AFBR. Moreover, the use of ME-FBR could be a convenient strategy for implementing of
347 MET for wastewater applications, as it is possible to overcome one of the main problems related
348 to these MET devices: low overall electric current for practical treatment uses due to electron
349 transfer limitations. Finally, the bioelectrochemical hydrogen generation by ME-FBR increases
350 the power capacity of biogas, making the technology more attractive to be implemented at higher
351 scale.

352

353 **Acknowledgement**

354 Financial support from the European Commission through the project ANSWER (Advanced
355 Nutrient Solutions With Electrochemical Recovery, LIFE Program, LIFE15/ENV/ES/00059)
356 is gratefully acknowledged.

357 **5. References**

358

359 [1] P. Weiland, Biogas production: Current state and perspectives, Appl. Microbiol.

- 360 Biotechnol. 85 (2010) 849–860. <https://doi.org/10.1007/s00253-009-2246-7>.
- 361 [2] W. Gujer, A.J.B. Zehnder, Conversion processes in anaerobic digestion, *Water Sci.*
362 *Technol.* 15 (1983) 127–167.
- 363 [3] L. Appels, J. Baeyens, J. Degève, R. Dewil, Principles and potential of the anaerobic
364 digestion of waste-activated sludge, *Prog. Energy Combust. Sci.* 34 (2008) 755–781.
365 <https://doi.org/10.1016/j.peecs.2008.06.002>.
- 366 [4] R. Rajagopal, D.I. Massé, G. Singh, A critical review on inhibition of anaerobic digestion
367 process by excess ammonia, *Bioresour. Technol.* 143 (2013) 632–641.
368 <https://doi.org/10.1016/j.biortech.2013.06.030>.
- 369 [5] K.H. Hansen, I. Angelidaki, B.K. Ahring, Anaerobic digestion of swine manure:
370 Inhibition by ammonia, *Water Res.* 32 (1998) 5–12. [https://doi.org/10.1016/S0043-](https://doi.org/10.1016/S0043-1354(97)00201-7)
371 [1354\(97\)00201-7](https://doi.org/10.1016/S0043-1354(97)00201-7).
- 372 [6] O. Yenigün, B. Demirel, Ammonia inhibition in anaerobic digestion: A review, *Process*
373 *Biochem.* 48 (2013) 901–911. <https://doi.org/10.1016/j.procbio.2013.04.012>.
- 374 [7] I. Angelidaki, B.K. Ahring, Thermophilic anaerobic digestion of livestock waste: the
375 effect of ammonia, *Appl. Microbiol. Biotechnol.* 38 (1993) 560–564.
376 <https://doi.org/10.1007/BF00242955>.
- 377 [8] S.A. Patil, F. Harnisch, B. Kapadnis, U. Schröder, Electroactive mixed culture biofilms in
378 microbial bioelectrochemical systems: The role of temperature for biofilm formation and
379 performance, *Biosens. Bioelectron.* 26 (2010) 803–808.
380 <https://doi.org/10.1016/j.bios.2010.06.019>.
- 381 [9] G.F. Parkin, W.F. Owen, Fundamentals of anaerobic digestion of wastewater sludges, *J.*
382 *Environ. Eng. (United States)*. 112 (1986) 867–920. [https://doi.org/10.1061/\(ASCE\)0733-](https://doi.org/10.1061/(ASCE)0733-9372(1986)112:5(867))
383 [9372\(1986\)112:5\(867\)](https://doi.org/10.1061/(ASCE)0733-9372(1986)112:5(867)).
- 384 [10] Y. Li, R. Zhang, G. Liu, C. Chen, Y. He, X. Liu, Comparison of methane production
385 potential, biodegradability, and kinetics of different organic substrates, *Bioresour.*
386 *Technol.* 149 (2013) 565–569. <https://doi.org/10.1016/j.biortech.2013.09.063>.

- 387 [11] R.M.W. Ferguson, F. Coulon, R. Villa, Organic loading rate: A promising microbial
388 management tool in anaerobic digestion, *Water Res.* 100 (2016) 348–356.
389 <https://doi.org/10.1016/j.watres.2016.05.009>.
- 390 [12] P.G. Kougias, T.A. Kotsopoulos, G.G. Martzopoulos, Effect of feedstock composition and
391 organic loading rate during the mesophilic co-digestion of olive mill wastewater and
392 swine manure, *Renew. Energy.* 69 (2014) 202–207.
393 <https://doi.org/10.1016/j.renene.2014.03.047>.
- 394 [13] K. Hwang, M. Song, W. Kim, N. Kim, S. Hwang, Effects of prolonged starvation on
395 methanogenic population dynamics in anaerobic digestion of swine wastewater,
396 *Bioresour. Technol.* 101 (2010). <https://doi.org/10.1016/j.biortech.2009.03.070>.
- 397 [14] T.G. Kim, T. Yi, J.-H. Lee, K.-S. Cho, Long-term survival of methanogens of an
398 anaerobic digestion sludge under starvation and temperature variation, *J. Environ. Biol.* 36
399 (2015) 371–375.
- 400 [15] J.J. Stone, S.A. Clay, G.M. Spellman, Tylosin and chlortetracycline effects during swine
401 manure digestion: Influence of sodium azide, *Bioresour. Technol.* 101 (2010) 9515–9520.
402 <https://doi.org/10.1016/j.biortech.2010.07.116>.
- 403 [16] J.-L. Xue, G.-M. Liu, D.-F. Zhao, J.-C.-Z. Li, X.-D. Su, Inhibition effects of
404 pentachlorophenol (PCP) on anaerobic digestion system, *Desalin. Water Treat.* 51 (2013)
405 5892–5897. <https://doi.org/10.1080/19443994.2013.803704>.
- 406 [17] J. De Vrieze, S. Gildemyn, J.B.A. Arends, I. Vanwonterghem, K. Verbeken, N. Boon, W.
407 Verstraete, G.W. Tyson, T. Hennebel, K. Rabaey, Biomass retention on electrodes rather
408 than electrical current enhances stability in anaerobic digestion, *Water Res.* 54 (2014)
409 211–221. <https://doi.org/10.1016/j.watres.2014.01.044>.
- 410 [18] Z. Zhao, Y. Zhang, L. Wang, X. Quan, Potential for direct interspecies electron transfer in
411 an electric-anaerobic system to increase methane production from sludge digestion, *Sci.*
412 *Rep.* 5 (2015). <https://doi.org/10.1038/srep11094>.
- 413 [19] H. Xu, K. Wang, D.E. Holmes, Bioelectrochemical removal of carbon dioxide
414 (CO₂): An innovative method for biogas upgrading, *Bioresour. Technol.* 173

- 415 (2014) 392–398. <https://doi.org/10.1016/j.biortech.2014.09.127>.
- 416 [20] S. Gajaraj, Y. Huang, P. Zheng, Z. Hu, Methane production improvement and associated
417 methanogenic assemblages in bioelectrochemically assisted anaerobic digestion, *Biochem.*
418 *Eng. J.* 117 (2017) 105–112. <https://doi.org/10.1016/j.bej.2016.11.003>.
- 419 [21] Y. Li, Y. Zhang, Y. Liu, Z. Zhao, Z. Zhao, S. Liu, H. Zhao, X. Quan, Enhancement of
420 anaerobic methanogenesis at a short hydraulic retention time via bioelectrochemical
421 enrichment of hydrogenotrophic methanogens, *Bioresour. Technol.* 218 (2016) 505–511.
422 <https://doi.org/10.1016/j.biortech.2016.06.112>.
- 423 [22] J. De Vrieze, J.B.A. Arends, K. Verbeeck, S. Gildemyn, K. Rabaey, Interfacing anaerobic
424 digestion with (bio)electrochemical systems: Potentials and challenges, *Water Res.* 146
425 (2018) 244–255. <https://doi.org/10.1016/j.watres.2018.08.045>.
- 426 [23] B.E. Logan, B. Hamelers, R. Rozendal, U. Schröder, J. Keller, S. Freguia, P. Aelterman,
427 W. Verstraete, K. Rabaey, Microbial fuel cells: Methodology and technology, *Environ.*
428 *Sci. Technol.* (2006). <https://doi.org/10.1021/es0605016>.
- 429 [24] B.E. Logan, *Microbial Fuel Cells*, 2008. <https://doi.org/10.1002/9780470258590>.
- 430 [25] B.E. Logan, M.J. Wallack, K.-Y. Kim, W. He, Y. Feng, P.E. Saikaly, Assessment of
431 Microbial Fuel Cell Configurations and Power Densities, *Environ. Sci. Technol. Lett.* 2
432 (2015) 206–214. <https://doi.org/10.1021/acs.estlett.5b00180>.
- 433 [26] V.G. Gude, Wastewater treatment in microbial fuel cells - An overview, *J. Clean. Prod.*
434 122 (2016) 287–307. <https://doi.org/10.1016/j.jclepro.2016.02.022>.
- 435 [27] S.K. Butti, G. Velvizhi, M.L.K. Sulonen, J.M. Haavisto, E. Oguz Koroglu, A. Yusuf
436 Cetinkaya, S. Singh, D. Arya, J. Annie Modestra, K. Vamsi Krishna, J.A. Puhakka, S.
437 Venkata Mohan, Microbial electrochemical technologies with the perspective of
438 harnessing bioenergy: Maneuvering towards upscaling, *Renew. Sustain. Energy Rev.* 53
439 (2016) 462–476. <https://doi.org/10.1016/j.rser.2015.08.058>.
- 440 [28] B.E. Logan, Scaling up microbial fuel cells and other bioelectrochemical systems, *Appl.*
441 *Microbiol. Biotechnol.* 85 (2010) 1665–1671. <https://doi.org/10.1007/s00253-009-2378-9>.

- 442 [29] D. Cecconet, D. Molognoni, A. Callegari, A.G. Capodaglio, Agro-food industry
443 wastewater treatment with microbial fuel cells: Energetic recovery issues, *Int. J. Hydrogen*
444 *Energy*. 43 (2018) 500–511. <https://doi.org/10.1016/j.ijhydene.2017.07.231>.
- 445 [30] P. Pandey, V.N. Shinde, R.L. Deopurkar, S.P. Kale, S.A. Patil, D. Pant, Recent advances
446 in the use of different substrates in microbial fuel cells toward wastewater treatment and
447 simultaneous energy recovery, *Appl. Energy*. 168 (2016) 706–723.
448 <https://doi.org/10.1016/j.apenergy.2016.01.056>.
- 449 [31] M.I. San-Martín, A. Sotres, R.M. Alonso, J. Díaz-Marcos, A. Morán, A. Escapa,
450 Assessing anodic microbial populations and membrane ageing in a pilot microbial
451 electrolysis cell, *Int. J. Hydrogen Energy*. 44 (2019) 17304–17315.
452 <https://doi.org/10.1016/j.ijhydene.2019.01.287>.
- 453 [32] Y. Zhang, I. Angelidaki, Microbial electrolysis cells turning to be versatile technology:
454 Recent advances and future challenges, *Water Res*. 56 (2014) 11–25.
455 <https://doi.org/10.1016/j.watres.2014.02.031>.
- 456 [33] T.H.J.A. Sleutels, A. Ter Heijne, C.J.N. Buisman, H.V.M. Hamelers, Bioelectrochemical
457 systems: An outlook for practical applications, *ChemSusChem*. 5 (2012) 1012–1019.
458 <https://doi.org/10.1002/cssc.201100732>.
- 459 [34] Z. Borjas, J.M. Ortiz, A. Aldaz, J.M. Feliu, A. Esteve-Núñez, Strategies for Reducing the
460 Start-up Operation of Microbial Electrochemical Treatments of Urban Wastewater,
461 *Energies*. 8 (2015) 14064–14077. <https://doi.org/10.3390/en81212416>.
- 462 [35] L.F. Leon-Fernandez, J. Villaseñor, L. Rodriguez, P. Cañizares, M.A. Rodrigo, F.J.
463 Fernández-Morales, Dehalogenation of 2,4-Dichlorophenoxyacetic acid by means of
464 bioelectrochemical systems, *J. Electroanal. Chem*. 854 (2019).
465 <https://doi.org/10.1016/j.jelechem.2019.113564>.
- 466 [36] S. Puig, M. Serra, M. Coma, M.D. Balaguer, J. Colprim, Simultaneous domestic
467 wastewater treatment and renewable energy production using microbial fuel cells (MFCs),
468 *Water Sci. Technol*. 64 (2011) 904–909. <https://doi.org/10.2166/wst.2011.401>.
- 469 [37] A. Iannaci, T. Pepè Sciarria, B. Mecheri, F. Adani, S. Licoccia, A. D’Epifanio, Power

- 470 generation using a low-cost sulfated zirconium oxide based cathode in single chamber
471 microbial fuel cells, *J. Alloys Compd.* 693 (2017) 170–176.
472 <https://doi.org/10.1016/j.jallcom.2016.09.159>.
- 473 [38] S. Mateo, M. Mascia, F.J. Fernandez-Morales, M.A. Rodrigo, M. Di Lorenzo, Assessing
474 the impact of design factors on the performance of two miniature microbial fuel cells,
475 *Electrochim. Acta.* 297 (2019) 297–306. <https://doi.org/10.1016/j.electacta.2018.11.193>.
- 476 [39] Y. Asensio, C.M. Fernandez-Marchante, J. Lobato, P. Cañizares, M.A. Rodrigo, Influence
477 of the fuel and dosage on the performance of double-compartment microbial fuel cells,
478 *Water Res.* 99 (2016) 16–23. <https://doi.org/10.1016/j.watres.2016.04.028>.
- 479 [40] Y. Asensio, I.B. Montes, C.M. Fernandez-Marchante, J. Lobato, P. Cañizares, M.A.
480 Rodrigo, Selection of cheap electrodes for two-compartment microbial fuel cells, *J.*
481 *Electroanal. Chem.* 785 (2017) 235–240. <https://doi.org/10.1016/j.jelechem.2016.12.045>.
- 482 [41] K. Scott, E.H. Yu, *Microbial Electrochemical and Fuel Cells: Fundamentals and*
483 *Applications*, 2015. <https://doi.org/10.1016/C2014-0-01767-4>.
- 484 [42] S. Tejedor-Sanz, J.M. Ortiz, A. Esteve-Núñez, Merging microbial electrochemical
485 systems with electrocoagulation pretreatment for achieving a complete treatment of
486 brewery wastewater, *Chem. Eng. J.* (2017). <https://doi.org/10.1016/j.cej.2017.08.049>.
- 487 [43] A. Deeke, T.H.J.A. Sleutels, T.F.W. Donkers, H.V.M. Hamelers, C.J.N. Buisman, A. Ter
488 Heijne, Fluidized capacitive bioanode as a novel reactor concept for the microbial fuel
489 cell, *Environ. Sci. Technol.* 49 (2015) 1929–1935. <https://doi.org/10.1021/es503063n>.
- 490 [44] S. Tejedor-Sanz, T. Bacchetti De Gregoris, J.J. Salas, L. Pastor, A. Esteve-Núñez,
491 Integrating a microbial electrochemical system into a classical wastewater treatment
492 configuration for removing nitrogen from low COD effluents, *Environ. Sci. Water Res.*
493 *Technol.* (2016). <https://doi.org/10.1039/c6ew00100a>.
- 494 [45] S. Tejedor-Sanz, J.R. Quejigo, A. Berná, A. Esteve-Núñez, The Planktonic Relationship
495 Between Fluid-Like Electrodes and Bacteria: Wiring in Motion, *ChemSusChem.* (2017).
496 <https://doi.org/10.1002/cssc.201601329>.
- 497 [46] S. Tejedor-Sanz, P. Fernández-Labrador, S. Hart, C.I. Torres, A. Esteve-Núñez, *Geobacter*

498 dominates the inner layers of a stratified biofilm on a fluidized anode during brewery
499 wastewater treatment, *Front. Microbiol.* (2018).
500 <https://doi.org/10.3389/fmicb.2018.00378>.

501 [47] J. Kan, L. Hsu, A.C.M. Cheung, M. Pirbazari, K.H. Neelson, Current production by
502 bacterial communities in microbial fuel cells enriched from wastewater sludge with
503 different electron donors, *Environ. Sci. Technol.* 45 (2011) 1139–1146.

504 [48] P.D. Kiely, R. Cusick, D.F. Call, P.A. Selembo, J.M. Regan, B.E. Logan, Anode microbial
505 communities produced by changing from microbial fuel cell to microbial electrolysis cell
506 operation using two different wastewaters, *Bioresour. Technol.* 102 (2011) 388–394.

507 [49] M.D. Yates, P.D. Kiely, D.F. Call, H. Rismani-Yazdi, K. Bibby, J. Peccia, J.M. Regan,
508 B.E. Logan, Convergent development of anodic bacterial communities in microbial fuel
509 cells, *ISME J.* 6 (2012) 2002–2013.

510 [50] P.M. Shrestha, A.-E. Rotaru, Plugging in or going wireless: strategies for interspecies
511 electron transfer, *Front. Microbiol.* 5 (2014) 237.

512 [51] A.-E. Rotaru, T.L. Woodard, K.P. Nevin, D.R. Lovley, Link between capacity for current
513 production and syntrophic growth in *Geobacter* species, *Front. Microbiol.* 6 (2015) 744.

514 [52] S. Kato, K. Hashimoto, K. Watanabe, Microbial interspecies electron transfer via electric
515 currents through conductive minerals, *Proc. Natl. Acad. Sci.* 109 (2012) 10042–10046.

516 [53] A.-E. Rotaru, P.M. Shrestha, F. Liu, T. Ueki, K. Nevin, Z.M. Summers, D.R. Lovley,
517 Interspecies electron transfer via hydrogen and formate rather than direct electrical
518 connections in cocultures of *Pelobacter carbinolicus* and *Geobacter sulfurreducens*, *Appl.*
519 *Environ. Microbiol.* 78 (2012) 7645–7651.

520 [54] C. Cruz Viggì, S. Rossetti, S. Fazi, P. Paiano, M. Majone, F. Aulenta, Magnetite particles
521 triggering a faster and more robust syntrophic pathway of methanogenic propionate
522 degradation, *Environ. Sci. Technol.* 48 (2014) 7536–7543.

523 [55] H. Li, J. Chang, P. Liu, L. Fu, D. Ding, Y. Lu, Direct interspecies electron transfer
524 accelerates syntrophic oxidation of butyrate in paddy soil enrichments, *Environ.*
525 *Microbiol.* 17 (2015) 1533–1547.

